

# Experimental and theoretical study of the mechanism for the kinetic of elimination of methyl carbazate in the gas phase

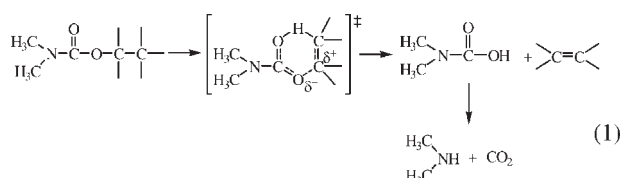
Armando Herize<sup>a</sup>, José R. Mora<sup>a</sup>, Jesus Lezama<sup>a</sup>, Edgar Marquez<sup>a</sup>, Tania Córdova<sup>b</sup> and Gabriel Chuchani<sup>a\*</sup>

The elimination kinetic of methyl carbazate in the gas phase was determined in a static system over the temperature range of 340–390 °C and pressure range of 47–118 Torr. The reaction is homogeneous, unimolecular, and obeys a first order rate law. The decomposition products are methyl amine, nitrous acid, and CO gas. The variation of the rate coefficients with temperatures is given by the Arrhenius expression:  $\log k_1$  ( $s^{-1}$ ) =  $(11.56 \pm 0.34) - (180.7 \pm 4.1) \text{ kJ mol}^{-1} (2.303 RT)^{-1}$ . The estimated kinetics and thermodynamics parameters are in good agreement to the experimental values using B3LYP/6-31G (d,p), and MP2/6-31G (d,p) levels of theory. These calculations imply a molecular mechanism involving a concerted non-synchronous quasi three-membered ring cyclic transition state to give an unstable intermediate, 1,2-oxaziridin-3-one. Bond order analysis and natural charges implies that polarization of O (alkyl)—C (alkyl) bond of the ester is rate determining in this reaction. Copyright © 2008 John Wiley & Sons, Ltd.

**Keywords:** kinetics; unimolecular elimination; pyrolysis; methyl carbazate; DFT and *ab initio* calculations

## INTRODUCTION

The elimination kinetics of *N,N*-dimethylcarbamates are known to proceed through a six-membered cyclic transition state type of mechanism similar to those described for acetates, carbonates, and xanthates<sup>[1–6]</sup> (reaction (1)).



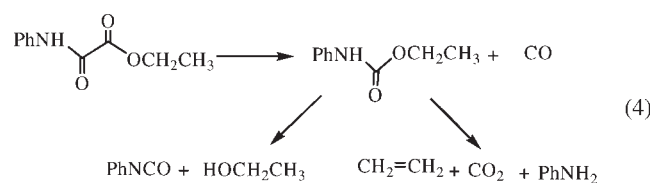
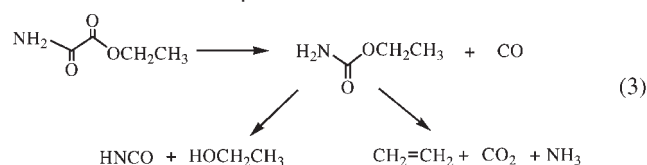
As in most organic esters, the presence of a  $C_{\beta}$ —H bond at the alkyl side of the ester for molecular elimination is necessary. However, when a  $\beta$ -hydrogen is absent at the alkyl group of esters, they are found to be stable above 500 °C and liable to undergo different type of reaction mechanisms according to their molecular structure.<sup>[2]</sup> In this sense, a carbamate such as methyl *N*-methylcarbamate,<sup>[7]</sup> with a hydrogen at the nitrogen atom and without a  $C_{\beta}$ —H bond at the alkyl side of the ester, yielded methyl isocyanate and methanol:



The mechanism of this reaction (2) was rationalized in terms of a four-membered cyclic transition state, where the H atom attached to nitrogen was considered to assist the elimination process (Scheme 1).<sup>[7]</sup>

Similarly, few thermal decomposition works<sup>[8,9]</sup> have described that the presence of a H atom at the nitrogen of primary alkyl carbamates, with or without  $C_{\beta}$ —H bond, lead to different

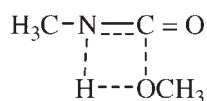
products formation to that described in reaction (1). This phenomenon is also shown in the gas phase elimination kinetics of the carbamate intermediate formed in the thermal decomposition of ethyl oxamate (reaction (3)) and ethyl oxalinate (reaction (4)).<sup>[10]</sup> Theoretical calculations for the mechanism of reactions (3) and (4)<sup>[11]</sup> were also reported.



\* Correspondence to: G. Chuchani, Centro de Química, Instituto Venezolano de Investigaciones Científicas (IVIC), Apartado 21827, Caracas, Venezuela. E-mail: chuchani@ivic.ve

a A. Herize, J. R. Mora, J. Lezama, E. Marquez, G. Chuchani  
Centro de Química, Instituto Venezolano de Investigaciones Científicas (IVIC), Apartado 21827, Caracas, Venezuela

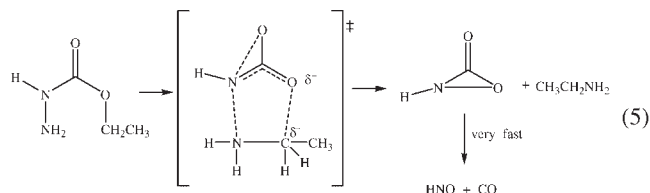
b T. Córdova  
Escuela de Química, Facultad de Ciencias, Universidad Central de Venezuela, Apartado 1020-A, Caracas, Venezuela



Scheme 1.

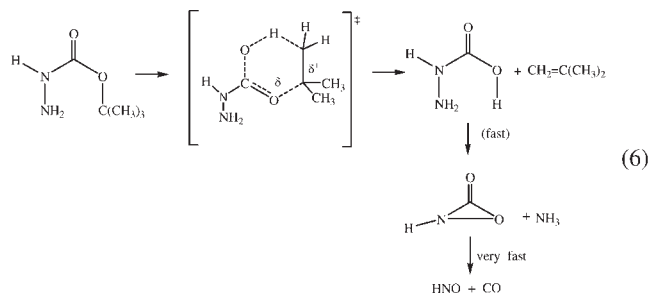
To avoid this type of elimination reaction, most gas phase pyrolysis of alkyl carbamates have been carried out with the hydrogens of the nitrogen substituent replaced by methyl or phenyl groups.<sup>[6,12–16]</sup>

An additional investigation, where one H of the nitrogen is replaced by NH<sub>2</sub> in carbamates, that is, ethyl carbamate,<sup>[17]</sup> (H<sub>2</sub>NNHCOOCH<sub>2</sub>CH<sub>3</sub>), was pyrolyzed in the gas phase to give ethyl amine, HNO, and CO gas (reaction (5)).



Theoretical calculations of the elimination kinetics of ethyl carbamate,<sup>[17]</sup> using the *ab initio* and *DFT* level of theories, showed the B3LYP/6-31G method to be in good agreement with the experimental results, suggesting reaction (5) as a reasonable mechanism.

In the case of *tert*-butyl carbamate,<sup>[17]</sup> reaction (6) is similar as to esters elimination of *N,N*-dimethylcarbamic acid (reaction (1)). The MP2/6-31G and MP2/6-31G\* levels of calculation are in good agreement with experimental and suggested a concerted, semi-polar six-membered cyclic transition state type of mechanism, approaching to planarity, where the bond polarization of O (alkyl)—C (alkyl) is rate determining.



In spite of the presence of a  $\beta$ -hydrogen at the alkyl side of ethyl carbamate, the mechanism and product formation shown in reaction (5) differs from the generally accepted elimination process as in carbamates described in reaction (1). This fact suggested to examine in the present work, both experimentally and theoretically, the gas phase elimination kinetic of a substrate without a  $\beta$ -hydrogen at the alkyl side and with the presence of a hydrogen attached to N such as methyl carbamate. Therefore, the purpose is to find whether methyl carbamate substrate proceeds according or different to reactions (2) or (5).

## COMPUTATIONAL METHOD AND MODEL

Calculations on the elimination kinetic of methyl carbamate have been carried out using MP2/6-31G(d,p), B3LYP/6-31G(d,p), and

MPW1PW91/6-31G(d,p) methods as implemented in Gaussian 98W.<sup>[18]</sup> The Bery analytical gradient optimization routines were used. The requested convergence on the density matrix was  $10^{-9}$  atomic units, the threshold value for maximum displacement was 0.0018 Å, and that for the maximum force was 0.00045 Hartree/Bohr. Transition state was performed using quadratic synchronous transit protocol as implemented in Gaussian 98W. The nature of stationary points was established by calculating and diagonalization of the Hessian matrix. The TS structure was characterized by means of normal-mode analysis. The unique imaginary frequency associated with the transition vector (TV), that is, the eigenvector associated with the unique negative eigenvalue of the force constant matrix has been identified and intrinsic reaction coordinate (IRC) calculations were performed to verify transition state structure.

Thermodynamic quantities such as zero point vibrational energy (ZPVE), temperature corrections ( $E(T)$ ) and absolute entropies ( $S(T)$ ), were obtained from frequency calculations and consequently, the rate coefficient can be estimated assuming that the transmission coefficient is equal to 1. Temperature corrections and absolute entropies were obtained assuming ideal gas behavior from the harmonic frequencies and moments of inertia by standard methods<sup>[19]</sup> at average temperature and pressure values within the experimental range. Scaling factors for frequencies and zero point energies for the methods used are taken from the literature.<sup>[20]</sup> In the case of *DFT* functional MPW1PW91 we used the same scaling factor suggested for B3LYP functional.

Method	$f_{\text{VIB}}$	$f_{\text{ZPE}}$
MPW1PW91/6-31G(d,p)	0.97	0.99
B3LYP/6-311G(d,p)	0.97	0.99
MP2(Full)/6-31G(d)	0.9427	0.9676

Rate coefficients  $k(T)$  were calculated using the TST<sup>[21–23]</sup> and assuming that the transmission coefficient is equal to 1.

$\Delta G^\ddagger$  was calculated using the Gibbs relations, and  $\Delta H^\ddagger$  was calculated using the following equation:

$$\Delta H^\ddagger = V^\ddagger + \Delta \text{ZPVE} + \Delta E(T)$$

where  $V^\ddagger$  is the potential energy barrier and  $\Delta \text{ZPVE}$  and  $\Delta E(T)$  are the differences of ZPVE and temperature corrections between the TS and the reactant, respectively. Entropy values were calculated from vibrational analysis and using Chuchani–Cordova idea of factor  $C^{\text{exp}}$ .<sup>[17]</sup> This factor has the purpose to rationalize the limitations of the theoretical methods since they do not consider the collisional entropy, only the analysis of a single molecule. In this respect, the theoretical estimations of  $\Delta G^{\text{theo}}$ ,  $\Delta S^{\text{theo}}$ , and  $\log A$  are generally far off from the experimental values. Therefore

$$\Delta H^{\text{exp}} \cong \Delta H^{\text{theo}} \text{ and consequently } E_a^{\text{exp}} \cong E_a^{\text{theo}},$$

$$\text{we expect that } \Delta G^{\text{exp}} \cong \Delta G^{\text{theo}}$$

$$\text{therefore } \Delta G^{\text{exp}} - E_a^{\text{exp}} = C^{\text{exp}},$$

$$\text{we obtain } \Delta G^{\text{theo}} = E_a^{\text{theo}} + C^{\text{exp}}$$

where the superscripts exp and theo refer to experimental and theoretical values, respectively and the parameter  $C^{\text{exp}}$  is

$$C^{\text{exp}} = nRT - \text{TDS}^{\text{exp}}, \quad n = 1 \quad \text{unimolecular reaction}$$

**Table 1.** Ratio of final ( $P_f$ ) to initial pressure ( $P_0$ ) of the substrate

Substrate	Temperature (°C)	$P_0$ (Torr)	$P_f$ (Torr)	$P_f/P_0$	Average
Methyl carbazate	349.8	47.6	139	2.9	2.95
	360.6	40.4	123	3.0	
	370.5	50.6	152	3.0	
	379.6	68	198	2.9	

$C^{\text{exp}}$  includes the contribution of collisional entropy which has not been considered in frequency calculations (isolated molecules).

Using  $\Delta G^{\# \text{theo}} = \Delta H^{\# \text{theo}} - T\Delta S^{\# \text{theo}}$ ,  $\Delta S^{\# \text{theo}}$  was obtained. From  $\Delta S^{\# \text{theo}}$ ,  $\Delta G^{\# \text{theo}}$ ,  $\log A$ , and the rate coefficients can be calculated.

## RESULTS AND DISCUSSIONS

The products formed from methyl carbazate decomposition in the gas phase are methyl amine, nitrous acid, and CO gas (reaction (7)).



The theoretical stoichiometry in reaction (7) for the molecular elimination of this substrate demands that the final pressure,  $P_f$ , be 3.0 times the initial pressure,  $P_0$ . The average experimental value of  $P_f/P_0$  at four different temperatures and 10 half-lives is 2.95 (Table 1).

The homogeneity of this reaction was established by carrying out several runs in a vessel with a surface to volume ratio of 6.0 relative to that of the normal vessel which is equal to 1.0 (Table 2). The packed and unpacked Pyrex vessel, seasoned with allyl

**Table 2.** Homogeneity of the elimination reaction at 370.6 °C

Substrate	$S/V$ ( $\text{cm}^{-1}$ ) <sup>a</sup>	$10^4 k_1$ ( $\text{s}^{-1}$ ) <sup>b</sup>	$10^4 k_1$ ( $\text{s}^{-1}$ ) <sup>c</sup>
Methyl carbazate	1	18.9 <sup>d</sup>	7.31
	6	27.4 <sup>d</sup>	7.88

<sup>a</sup>  $S$  = surface area;  $V$  = volume.

<sup>b</sup> Clean pyrex vessel.

<sup>c</sup> Vessel seasoned with allyl bromide.

<sup>d</sup> Average of several runs.

bromide, had no effect on rates. However, the packed and unpacked clean Pyrex vessel resulted in some significant heterogeneous effect in the rate coefficients.

The pyrolysis experiment was carried out in the presence of the free radical suppressor toluene in order to prevent any possible chain reaction. The effect of different proportions of toluene in the elimination process is shown in Table 3. No induction period was observed. The rate coefficient was reproducible with a relative deviation less than 5% at a given temperature.

The first-order rate coefficient of the carbazate, calculated from  $k_1 = (2.303/t) \log (2P_0)/(3P_0 - P_f)$  was found to be independent of the initial pressure (Table 4). A plot of  $\log (2P_0 - P_f)$  against time  $t$  gave a good straight line up to 65% reaction. The variations of the rate coefficients with temperature are shown in Table 5. The results given in Table 5 lead, by using the least squares procedure and 90% confidence limits, to the shown Arrhenius equation.

From the results given in Table 6, a theoretical calculation was carried out in order to suggest a reasonable mechanism of elimination of methyl carbazate described in reaction (7).

## THEORETICAL RESULTS

The gas-phase elimination reaction of methyl carbazate gave methylamine, HNO, and CO, according to reaction (7). The products from mechanism (2) are  $\text{NH}_2\text{NCO}$  and methanol, however, these were not observed. Conversely, mechanism (5) is consistent with the formation of the products obtained experimentally, methylamine, HNO, and CO.

The theoretical calculations of mechanism (5) were carried out based on the assumption that the reaction occurs in a two step process. In a first rate-determining step methyl carbazate eliminates rendering products methylamine and an unstable cyclic intermediate 1,2-oxaziridin-3-one, COONH, which rapidly decomposes to give HNO and CO.

The TS structure for the rate-determining step was found to be similar to the proposed intermediate, as shown in Fig. 1.

**Table 3.** Effect of free radical inhibitor toluene on rates<sup>a</sup>

Substrate	Temperature (°C)	$P_s$ (Torr)	$P_i$ (Torr)	$P_f/P_s$	$10^4 k_1$ ( $\text{s}^{-1}$ )
Methyl carbazate	370.5	62	—	—	8.11
		125	77	0.6	7.72
		134	109	0.8	7.58
		73	153	2.1	7.11
		47	183	3.9	7.68

<sup>a</sup> Seasoned vessel.  $P_s$  = pressure substrate.  $P_i$  = pressure inhibitor.

**Table 4.** Invariability of the rate coefficients with initial pressure

Substrate	Temperature (°C)	Parameters	Value			
Methyl carbazate	370.5	$P_0$ (Torr)	47	73	91	118
		$10^4 k_1$ (s <sup>-1</sup> )	7.68	7.11	7.11	7.00

**Table 5.** The variation of the rate coefficients with temperatures

Substrate	Parameters	Value					
Methyl carbazate	Temperature (°C)	340.9	349.8	360.9	370.8	379.6	389.8
	$10^4 k_1$ (s <sup>-1</sup> )	1.56	2.72	4.52	7.61	12.72	22.04

Rate equation  $\log k_1$  (s<sup>-1</sup>) = (11.56 ± 0.34) - (180.7 ± 4.1) kJ mol<sup>-1</sup> (2.303 RT)<sup>-1</sup>,  $r = 0.9990$ .

**Table 6.** Kinetic and thermodynamic parameters at 370 °C

Substrate	$k_1 \times 10^4$ (s <sup>-1</sup> )	$E_a$ (kJ/mol)	$\log A$ (s <sup>-1</sup> )	$\Delta S^\ddagger$ (J/mol K)	$\Delta H^\ddagger$ (kJ/mol)	$\Delta G^\ddagger$ (kJ/mol)
Methyl carbazate	7.98	180.7 ± 4.1	11.56 ± 0.34	-38.3	175.3	200.0

The TS was verified by IRC calculations. The TS is late in the reaction coordinate, as illustrated in Fig. 2. The IRC calculation gave a configuration for the reactant that is higher in energy than the optimized reactant, suggesting that the substrate adopts a reactive-high energy conformation prior to the reaction.

Geometries for reactant, TS, and products for the rate-determining step were optimized by means of the methods described in Table 7. The decomposition rate for the 1,2-oxaziridin-3-one intermediate using B3LYP/6-31G(d,p) was found to be very rapid compared to the previous step as seen in last entry in Table 7.

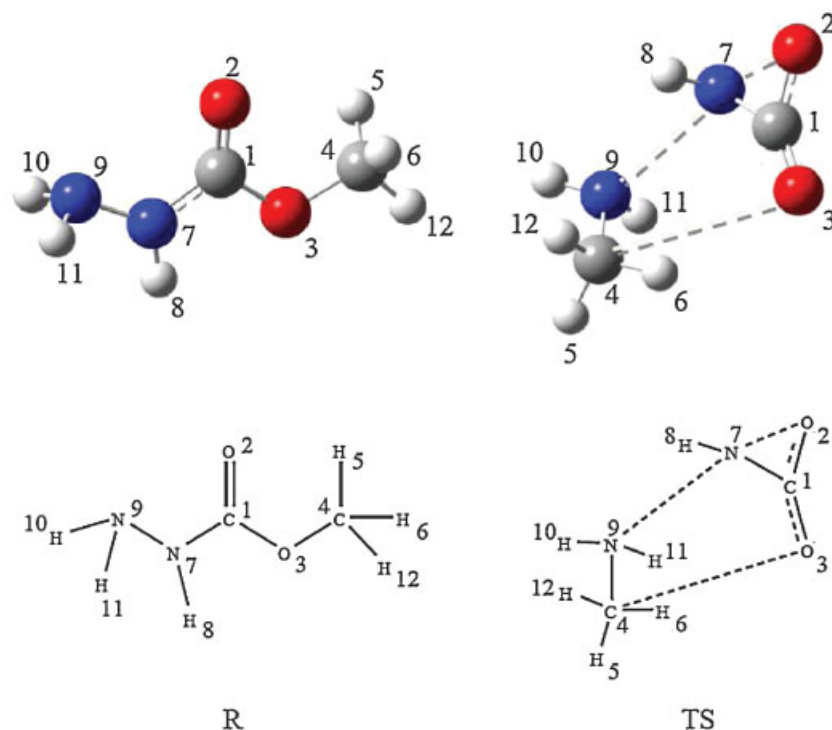


**Figure 1.** Reactant (left) and transition state TS (right) optimized at B3LYP/6-31G(d,p) level of theory. Schematic drawings with atom numbers are given for clarity

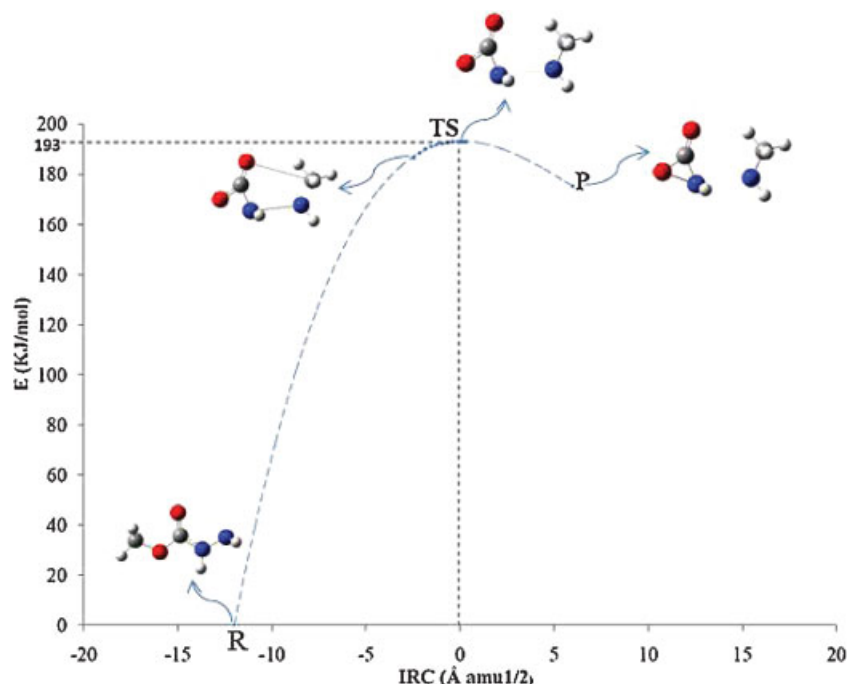


**Figure 2.** Intrinsic reaction coordinate (IRC) for the gas phase elimination kinetics of methyl carbazate at B3LYP/6-31G(d,p). The configuration of the reactant obtained by the IRC calculations is of higher energy than the optimized reactant, thus suggesting that the reactant undergoes a conformational change to reach the TS configuration

The results obtained using B3LYP/6-31G (d,p), and MP2/6-31G (d,p) levels of theory were found to be in a reasonable agreement with the experimental values (Table 7). By using factor  $C = 19.3$  it is possible to have a better estimate of the kinetic and thermodynamic parameters (Table 8).

The geometrical parameters for the TS confirm the similarity to the proposed intermediate (Table 9). The O—C ester bond is about broken showing a distance  $O_3—C_4$  of 3.480. Conversely,

the distance  $O_2—N_7$  is shortened to 1.670 Å in an almost closed configuration of the 1,2-oxaziridin-3-one intermediate. Changes in hybridization and bond orders are reflected in distances  $C_1—O_2$  and  $C_1—O_3$ . Atoms  $C_1$ ,  $O_2$ ,  $N_7$  are positioned in a three-member like structure. Substantial progress is also observed in  $N_7—N_9$  bond breaking (2.55 Å in TS). Bond angles and dihedrals characterizing the TS geometry are also shown (Table 9). The unique imaginary frequency is identified.

**Table 7.** Kinetic and thermodynamic parameters for elimination at 643 K (370 °C)

Methods	$10^4 k$ (s <sup>-1</sup> )	$E_a$ (kJ mol <sup>-1</sup> )	Log A	$\Delta S^\ddagger$ (J mol <sup>-1</sup> K <sup>-1</sup> )	$\Delta H^\ddagger$ (kJ mol <sup>-1</sup> )	$\Delta G^\ddagger$ (kJ mol <sup>-1</sup> )
Experimental	7.98	180.7	11.56	-38.3	175.3	200.0
B3LYP/6-31G(d,p)	4260	187.9	14.9	25.0	182.6	166.4
MP2/6-31G(d,p)	4260	187.9	14.9	25.0	182.6	166.4
MPW1PW91/6-31G(d,p)	8200	207.6	15.1	28.6	169.0	150.6
B3LYP/6-31G(d,p) <sup>a</sup>	4420 000	90.4	14.0	8.0	85.1	79.9

<sup>a</sup> Fast step.

**Table 8.** Calculated kinetic and thermodynamic parameters obtained for the elimination reaction of methyl carbazate at 643 K (370 °C) using factor  $C^{\text{exp}} = 19.3$

Methods	$10^4 k$ (s <sup>-1</sup> )	$E_a$ (kJ mol <sup>-1</sup> )	Log A	$\Delta S^\ddagger$ (J mol <sup>-1</sup> K <sup>-1</sup> )	$\Delta H^\ddagger$ (kJ mol <sup>-1</sup> )	$\Delta G^\ddagger$ (kJ mol <sup>-1</sup> )
Experimental	7.98	180.7	11.56	-38.3	175.3	200.0
B3LYP/6-31G(d,p)	2.01	187.9	11.57	-38.2	182.6	207.2
MP2/6-31G(d,p)	2.01	187.9	11.57	-38.2	182.6	207.2

**Table 9.** Structural parameters of methyl carbazate elimination

		Bond length (Å)							
		C <sub>1</sub> -O <sub>2</sub>	C <sub>1</sub> -O <sub>3</sub>	O <sub>2</sub> -N <sub>7</sub>	O <sub>3</sub> -C <sub>4</sub>	C <sub>4</sub> -N <sub>9</sub>	N <sub>7</sub> -N <sub>9</sub>		
	R	1.210	1.360	2.310	1.430	4.720	1.380		
	TS	1.309	1.190	1.670	3.480	1.460	2.550		
	P	1.327	1.190	1.620	4.280	1.470	2.880		
		Bond angles							
		O <sub>2</sub> -C <sub>1</sub> -O <sub>3</sub>	O <sub>2</sub> -C <sub>1</sub> -N <sub>7</sub>		N <sub>7</sub> -C <sub>1</sub> -O <sub>3</sub>				
	R	124.722	127.550		107.720				
	TS	140.700	76.410		142.830				
	P	140.361	73.300		146.320				
		Dihedral angles							
		O <sub>2</sub> -C <sub>1</sub> -O <sub>3</sub> -C <sub>4</sub>	C <sub>1</sub> -O <sub>3</sub> -C <sub>4</sub> -N <sub>9</sub>	O <sub>3</sub> -C <sub>4</sub> -N <sub>9</sub> -N <sub>7</sub>	C <sub>4</sub> -N <sub>9</sub> -N <sub>7</sub> -C <sub>1</sub>	N <sub>9</sub> -N <sub>7</sub> -C <sub>1</sub> -O <sub>2</sub>	N <sub>9</sub> -N <sub>7</sub> -O <sub>2</sub> -O <sub>3</sub>	N <sub>9</sub> -N <sub>7</sub> -C <sub>1</sub> -O <sub>3</sub>	N <sub>9</sub> -N <sub>7</sub> -C <sub>1</sub> -O <sub>3</sub>
TS	157.460	27.422	-18.520	20.860	-163.830	-177.800	18.450	18.450	
TS vibrational frequency (cm <sup>-1</sup> )				97.1					

B3LYP/6-31G(d,p) method. Atom distances in Å and Dihedral angles in degrees.

**Table 10.** NBO charges of reactants and TS for methyl carbazate elimination at B3LYP/6-31G(d,p) level

	NBO charges		
	R	TS	P
C <sub>1</sub>	0.809	0.748	0.732
O <sub>2</sub>	-0.492	-0.378	-0.369
O <sub>3</sub>	-0.503	-0.444	-0.433
C <sub>4</sub>	-0.070	-0.201	-0.199
N <sub>7</sub>	-0.476	-0.307	-0.362
N <sub>9</sub>	-0.422	-0.612	-0.633

Calculated NBO charges are given in (Table 10). The most important changes in electron distribution are reflected in changes in atoms O<sub>3</sub> and C<sub>4</sub>. There is an increase in partial charge on C<sub>4</sub> (from -0.070 to -0.201 in TS, implying C<sub>4</sub> becoming more positive), while O<sub>3</sub> depict less negative charge. Nitrogen N<sub>7</sub> possess less negative charge in the TS compared to reactants (-0.476 to -0.307 in TS) whereas nitrogen N<sub>9</sub> increases its negative

charge (-0.422 to -0.612). The electron distribution in the TS is similar to that of the intermediate product.

#### Bond order analysis

Bond order analysis has been used successfully to describe reaction changes. Bond order calculations NBO were performed.<sup>[24–26]</sup> Wiberg bond indexes<sup>[27]</sup> were computed using the natural bond orbital NBO program<sup>[28]</sup> as implemented in Gaussian 98W. The process of bond breaking and bond formation involved in the reaction mechanism can be monitored by means of the Synchronicity (Sy) concept proposed by Moyano *et al.*<sup>[29]</sup> defined by the expression:

$$Sy = 1 - \frac{[\sum_{i=1}^n |\delta B_i - \delta B_{av}| / \delta B_{av}]}{2n - 2}$$

$n$  represents the number of bonds directly involved in the reaction and the relative variation of the bond index is obtained from

$$\delta B_i = \frac{[B_i^{TS} - B_i^R]}{[B_i^P - B_i^R]}$$

**Table 11.** NBO analysis of methyl carbazate thermal decomposition

	C <sub>1</sub> -O <sub>2</sub>	C <sub>1</sub> -O <sub>3</sub>	O <sub>2</sub> -N <sub>7</sub>	O <sub>3</sub> -C <sub>4</sub>	C <sub>4</sub> -N <sub>9</sub>	N <sub>7</sub> -N <sub>9</sub>	$\delta B_{av}$	Sy
B <sub>i</sub> <sup>R</sup>	1.6961	0.9646	0.1433	0.8862	0.0020	1.0412	0.9507	0.9745
B <sub>i</sub> <sup>TS</sup>	1.0985	1.7749	0.8298	0.0028	1.0077	0.0914		
B <sub>i</sub> <sup>P</sup>	1.0310	1.7996	0.9133	0.0003	1.0017	0.0315		
%E <sub>v</sub>	89.85	97.04	89.16	99.72	100.60	94.07		

Wiberg bond indexes (B<sub>i</sub>), % evolution through the reaction coordinate (%E<sub>v</sub>), average bond index variation ( $\delta B_{av}$ ) and synchronicity parameter (Sy). B3LYP/6-31G(d,p) level of theory.

where the superscripts R, TS, P, represent reactant, transition state, and product, respectively. The evolution in bond change is calculated as:

$$\%E_v = \delta B_i \times 100$$

The average value is calculated from

$$\delta B_{\text{ave}} = \frac{1}{n \sum_{i=1}^n \delta B_i}$$

Bonds indexes were calculated for those bonds involved in the reaction changes, that is, C<sub>1</sub>—O<sub>2</sub>, C<sub>1</sub>—O<sub>3</sub>, O<sub>2</sub>—N<sub>7</sub>, O<sub>3</sub>—C<sub>4</sub>, C<sub>4</sub>—N<sub>9</sub>, N<sub>7</sub>—N<sub>9</sub>. The remaining bonds stay practically unaltered during the process.

The analysis of bonds orders and changes from NBO calculations are described in Table 11. The evolution observed for all bonds imply a late TS with bonds being similar to those in the intermediate. The Synchronicity parameter Sy = 0.9745 suggests a concerted non-synchronic mechanism.

## CONCLUSIONS

The kinetics study of the gas-phase elimination reaction of methyl carbazate, reveal that the process is homogeneous, unimolecular, and it obeys a first-order rate law. The option of mechanism (2) is not possible in view of the products observed experimentally. Theoretical calculations on methyl carbazate thermal decomposition are based on the assumption that the reaction occurs in a two-step process (reaction (5)), involving an unstable three-membered ring intermediate, 1,2-oxaziridin-3-one. The transition state configuration is late in the reaction coordinate, being a quasi-cyclic structure similar to the proposed intermediate 1,2-oxaziridin-3-one. The results imply a concerted non-synchronous mechanism, through a quasi-three-membered ring transition state. Structural parameters, partial charges and NBO analysis suggest that bond polarization of O<sub>3</sub>—C<sub>4</sub> bond is the determining factor in the decomposition process. The synchronicity parameter Sy = 0.9745 suggests a less polarized TS compared to ethyl carbazate (Sy = 0.731), however a similar TS structure is observed. The Sy value suggests a concerted non-synchronic polar type of mechanism. A reasonable agreement of activation parameters with experimental parameters was found for B3LYP/6-31G (d,p) and MP2/6-31G (d,p) levels of theory.

## EXPERIMENTAL

Methyl carbazate was acquired from ACROS and after distillation to better than 98.5% purity (GC/MS (Saturn 2000, Varian) Capillary column DB-5MS, 30 m × 0.250 mm, i.d. 0.25 μm) was used. The product CH<sub>3</sub>NH<sub>2</sub> reacts with the HNO to form a solid CH<sub>3</sub>NH<sub>3</sub><sup>+</sup> NO<sup>-</sup> in the trap of the reaction vessel. This salt was identified by Mass Spectroscopy. The free amine was obtained through a column of soda lime and analyzed by using an HP 5710A gas chromatograph with a Porapak (80–100 mesh) column.

### Kinetics

The kinetics determinations were performed in a static system as reported before.<sup>[30–32]</sup> The rate coefficients were calculated from pressure increase measured manometrically. The temperature was controlled by a resistance thermometer controller and an

Omega Model SSR280A45 solid-state relay, maintained within ±0.2 °C and measured with a calibrated platinum–platinum 13% rhodium thermocouple with an Omega DP41-TC/DP41-RTD high performance digital temperature indicator. No temperature gradient was detected along the reaction vessel. The substrate was dissolved in benzyl alcohol and injected directly into the reaction vessel with a syringe through a silicone rubber septum. The amount of substrates used for each run was ~0.05–0.1 ml.

## REFERENCES

- [1] N. J. Daly, F. Ziolkowski, *Aust. J. Chem.* **1971**, *24*, 2541–2546.
- [2] R. Taylor, *The Chemistry of Functional Group Supplementary. Volume B, Acid Derivatives* (Ed.: S. Patai), Wiley, Chichester, **1979**; 859–914, Chapter 15.
- [3] K. A. Holbrook, *The Chemistry of Acids Derivatives, Volume 2, Vapor and Gas Phase Reactions of Carboxylic Acids and Their Derivatives* (Ed.: S. Patai), Wiley, Chichester, **1992**; 703–746, Chapter 12.
- [4] G. G. Smith, K. I. Voorkees, F. M. Kelly, *J. Chem. Soc. Chem. Commun.* **1971**, 789–790.
- [5] A. S. Gordon, W. P. Norris, *J. Phys. Chem.* **1965**, *69*, 3013–3017.
- [6] H. Kwart, J. Slutsky, *J. Chem. Soc. Chem. Commun.* **1972**, 552–553.
- [7] N. J. Daly, F. Ziolkowski, *Aust. J. Chem.* **1972**, *25*, 1453–1458.
- [8] V. Y. Bordzilovkii, B. M. Sadinov, A. G. Sutulo, *J. Appl. Chem. USSR* **1992**, *65*, 145–149.
- [9] R. Taylor, *J. Chem. Soc. Perkin Trans. II* **1975**, 1025–1029.
- [10] E. V. Chacin, M. Tosta, A. Herize, R. M. Domínguez, Y. Alvarado, G. Chuchani, *J. Phys. Org. Chem.* **2005**, *18*, 539–545.
- [11] J. R. Mora, M. Loroño, T. Cordova, G. Chuchani, *J. Phys. Org. Chem.* **2006**, *19*, 503–511.
- [12] H. Kwart, J. Slutsky, *J. Chem. Soc. Chem. Commun.* **1972**, 1182–1183.
- [13] N. J. Daly, F. Ziolkowski, *J. Chem. Soc. Chem. Commun.* **1972**, 911–912.
- [14] M. Luiggi, R. M. Domínguez, A. Rotinov, A. Herize, M. Cordova, G. Chuchani, *Int. J. Chem. Kinet.* **2002**, *34*, 1–5.
- [15] G. Chuchani, O. Nuñez, N. Marcano, S. Napolitano, H. Rodríguez, M. Domínguez, J. Ascanio, A. Rotinov, R. M. Domínguez, A. Herize, *J. Phys. Org. Chem.* **2001**, *14*, 146–158.
- [16] G. Chuchani, R. M. Domínguez, A. Rotinov, A. Herize, *J. Phys. Org. Chem.* **1999**, *16*, 40–46.
- [17] A. Rotinov, R. M. Domínguez, T. Cordova, G. Chuchani, *J. Phys. Org. Chem.* **2005**, *18*, 616–624.
- [18] M. J. Frisch, G. W. Trucks, H. B. Schlegel, G. E. Scuseria, M. A. Robb, J. R. Cheeseman, V. G. Zakrzewski, J. A. Montgomery, Jr., R. E. Stratmann, J. C. Burant, S. Dapprich, J. M. Millam, A. D. Daniels, K. N. Kudin, M. C. Strain, O. Farkas, J. Tomasi, V. Barone, M. Cossi, R. Cammi, B. Mennucci, C. Pomelli, C. Adamo, S. Clifford, J. Ochterski, G. A. Petersson, P. Y. Ayala, Q. Cui, K. Morokuma, D. K. Malick, A. D. Rabuck, K. Raghavachari, J. B. Foresman, J. Cioslowski, J. V. Ortiz, B. B. Stefanov, G. Liu, A. Liashenko, P. Piskorz, I. Komaromi, R. Gomperts, R. L. Martin, D. J. Fox, T. Keith, M. A. Al-Laham, C. Y. Peng, A. Nanayakkara, C. Gonzalez, M. Challacombe, P. M. W. Gill, B. Johnson, W. Chen, M. W. Wong, J. L. Andres, C. Gonzalez, M. Head-Gordon, ES Replogle, JA Pople, *Gaussian 98, Revision A.3*, Gaussian Inc., Pittsburgh, PA, **1998**.
- [19] D. McQuarrie, *Statistical Mechanics*, Harper & Row, New York, **1986**.
- [20] J. B. Foresman, A. Frish, *Exploring Chemistry with Electronic Methods* (2nd edn), Gaussian Inc, Pittsburg, PA, **1996**.
- [21] S. W. Benson, *The Foundations of Chemical Kinetics*, Mc-Graw-Hill, New York, **1960**.
- [22] H. E. O'Neal, S. W. Benson, *J. Phys. Chem.* **1967**, *71*, 2903–2921.
- [23] S. W. Benson, *Thermochemical Kinetics*. John Wiley & Sons, New York, **1968**.
- [24] G. J. Lendvay, *J. Phys. Chem.* **1989**, *93*, 4422–4429.
- [25] A. E. Reed, R. B. Weinstock, F. Weinhold, *J. Chem. Phys.* **1985**, *83*(2), 735–746.
- [26] A. E. Reed, L. A. Curtiss, F. Weinhold, *Chem. Rev.* **1988**, *88*, 899–926.
- [27] K. B. Wiberg, *Tetrahedron*, **1968**, *24*, 1083–1095.
- [28] E. D. Glendening, A. E. Reed, J. E. Carpenter, F. Weinhold, *NBO version 3.1*.
- [29] A. Moyano, M. A. Periclas, E. Valenti, *J. Org. Chem.* **1989**, *54*, 573–582.
- [30] A. Maccoll, *J. Chem. Soc.* **1955**, 965–973.
- [31] E. S. Swinbourne, *Aust. J. Chem.* **1958**, *11*, 314–330.
- [32] R. M. Domínguez, A. Herize, A. Rotinov, A. Alvarez-Aular, G. Visbal, G. Chuchani, *J. Phys. Org. Chem.* **2004**, *17*, 399–408.